ISSN 0001-4370, Oceanology, 2016, Vol. 56, No. 5, pp. 721–732. © Pleiades Publishing, Inc., 2016.
Original Russian Text © Al.A. Schreider, A.A. Schreider, A.E. Sazhneva, V.A. Sychev, O.A. Zuev, 2016, published in Okeanologiya, 2016, Vol. 56, No. 5, pp. 791–803.

MARINE GEOLOGY

# Kinematics of the Bottom of the Eurasia Basin Near the Spitsbergen Domain

**Al. A. Schreider[a], A. A. Schreider[b], A. E. Sazhneva[b], V. A. Sychev[b], and O. A. Zuev[c]**

[a] *Research Institute of Economics and Management in the Gas Industry Ltd, Moscow, Russia*
[b] *Shirshov Institute of Oceanology, Russian Academy of Sciences, Moscow, Russia*
[c] *Moscow Physical–Technical Institute, Moscow, Russia*
*e-mail: aschr@ocean.ru*

Received November 18, 2014; in final form, February 19, 2015

**Abstract**—Prior to extension of the lithosphere in the Eurasia Basin, the Yermak Plateau was an element of the Eurasian Arctic margin. Extension of the Barents Sea shelf culminated gradually in rifting of the continental crust with separation of this block from the continent during Chrons C25r–C26n (57.656–59.237 Ma ago) and emplacement of numerous basic dikes, which could be responsible for the formation of high-amplitude magnetic anomalies on the Yermak Plateau. The investigation included reconstruction of axes in the breakup zones along peripheral continental fragments of Spitsbergen with determination of the Euler poles and angles of rotation, which describe the kinematics of this process. It is revealed that the difference between depths of conjugate isobaths can be as large as many tens of meters, which reflects the nonuniformly scaled slide of peripheral areas of the continental crust along the plane of the crustal-penetrating fault and, correspondingly, their different subsidence during rifting.

**DOI:** 10.1134/S000143701604010X

## INTRODUCTION

Reconstruction of the paleogeodynamic evolution of the Arctic Ocean is among the most important problems in studying the Arctic region. Its origin and tectonic development remain a debatable topic in many publications [3, 4, 6, 8, 9, 22, 23, 32, 35, etc.].

Particular attention is devoted to the Eurasia Basin with its active mid-ocean (Mid-Arctic) ridge, the single such structure in the Arctic Ocean. The Eurasia Basin comprises four deep-sea basins: the Amundsen (between the Lomonosov Ridge and axis of the Mid-Arctic Ridge), Lincoln (between the Morris Jesup Rise and Lomonosov Ridge), Nansen (between the spreading axis of the Mid-Arctic Ridge and Eurasian shelf), and Sophia (between the Yermak Plateau and Spitsbergen). Geological and geophysical investigations of the Eurasia Basin in the Spitsbergen Archipelago area, which includes the Yermak Plateau, Sophia Basin, and adjacent areas, play an important role in reconstructing the stages in the formation of the Eurasia Basin.

The investigations carried out by the international scientific community during the last half-century yielded information on the bottom topography, sedimentary cover, crust structure, and anomalous potential fields of the Eurasia Basin near the Spitsbergen domain. At the same time, it should be noted that the ice cover of the Arctic Ocean including areas adjacent to Spitsbergen hampers gathering of information on the geological structure of its bottom. It is frequently impossible to discriminate between bedrock fragments and ice-rafted material among geological samples obtained by research vessels from the bottom. The ice cover also limits the possibilities for obtaining geological data by deep-sea drilling. Therefore, comprehensive analysis of the available geological and geophysical data is important, which will make it possible to clarify several important aspects about the stages in the geological development of the segment of the Eurasia Basin adjacent to Spitsbergen. This is the aim of this work.

## GEOLOGICAL AND GEOPHYSICAL DATA

The polar Spitsbergen Archipelago is located on the Eurasian shelf of the Arctic Ocean between 76°26′ and 80°50′ N and 10° and 32° E. It is characterized by a mountainous relief and shores with numerous fjords. The highest summit of the islands is located at an altitude of 1712 m in western Spitsbergen. The Spitsbergen domain adjacent to the Eurasia Basin of the Arctic Ocean has no distinct geographical boundaries. In this work, it is considered within a sector with coordinates of 80°–83° N and 5°–25° E (Fig. 1).

Water depths (according to [39]) in the Nansen Basin adjacent to the Spitsbergen domain exceed 3.5 km, while in east Sophia Basin, they never exceed 2.5 km, gradually decreasing in to the west up to 1 km

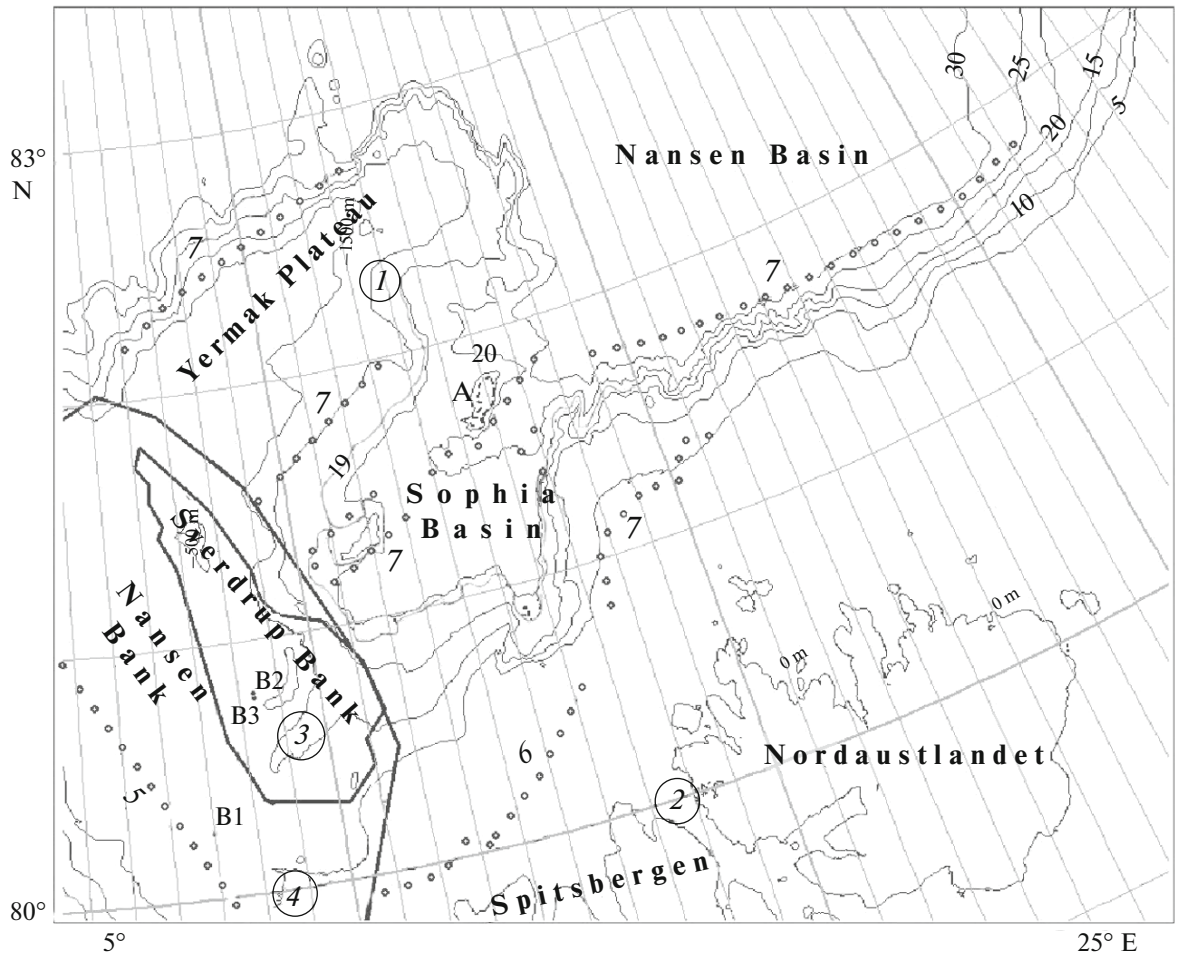


**Fig. 1.** Bathymetric map of the Eurasia Basin near the Spitsbergen domain, after [39] with location of rise A, deep-sea drilling sites B1–B3 [28], and troughs (in parentheses): (*1*) Litke [14]. (*2*) Khinlopen [15]. (*3*) Sophia [14], (*4*) Danskoya Basin-Trough [14]. Dashed lines indicate faults: (*5*) Hornsand [15], (*6*) Moffen, (*7*) unnamed tectonic fractures (faults) [15]. Contours of Sverdrup and Nansen banks are shown by solid lines [14, 15].

or shallower. The average width of the Sophia Basin in its central part is approximately 150 km.

The westernmost part of the basin, where the shallow-water part of the undersea Spitsbergen margin joins the Yermak Plateau, hosts the sublatitudinal Sophia Canyon ([14, etc.]), which can serves as their tectonic boundary. The canyon is approximately 1500 m deep in its eastern part and around 30 km wide. Its water depths decrease from shelf values west toward the Nansen Bank, defined at the junction of Spitsbergen with the Yermak Plateau (according to other data, e.g., [15], this area is occupied by the Sverdrup Bank, which partly overlaps the Nansen Bank and includes the Sophia Trough). In its eastern part, the basin hosts an isolated unnamed seamount with a summit depth shallower than 1 km; for convenience, we call it rise A.

The southern shelf of the Sophia Basin on the Spitsbergen side is bordered by the Danskoya Basin, which represents, according to [14, 30], a narrow trough approximately 15 km wide. To the east, the trough grades into a submarine continuation of the Woodfjorden with an incision depth up to 250 m and a width of 20 km.

Further east, there is a narrow (15 km) spur approximately 50 km long, which separates some areas of the basin with water depths up to 2 km from its main part. The shelf continuation of this separated area of the basin is intersected by a fjord separating Nordaustlandet and the Spitsbergen islands and representing a trough 25 km wide with an incision depth up to 200 m, which is intersected by the Moffen Fault.

The surface of the Yermak Rise (Plateau) located along the northern slope of the Sophia Basin is characterized by nonuniform patterns. Its easternmost part, up to 60 km wide, is located at water depths of 1.5 km. It continues westward for 100 km along the inner margin of the Sophia Basin in the form of a plateau bench up to 40 km wide. This area is separated from the central part of the rise by a trough with steep walls and a complex sigmoid configuration. The latter

most likely reflects subvertical tectonic displacement with an amplitude exceeding 0.5 km and in its southern part is called the Litke Trough [14]. The central part of the Yermak Plateau is located at water depths of approximately 0.7 km, characterized by a system of trough-shaped structures up to several kilometers wide and with a relative incision up to tens of meters. To the west, the surface of the plateau rises up to water depths of 0.5 km and joins, via the Nansen Bank, the submarine margin of Spitsbergen. In a deep-sea drilling project, several holes were drilled at three sites (910–912 [27]) on the Yermak Plateau adjacent to the Spitsbergen domain by the D/V *JOIDES Resolution* in 1993. All of them penetrated the Pliocene–Quaternary sedimentary sequence, which is subdivided, based on their composition and physical properties, into subunits 1A–1C.

Site 910 (Holes 910A–910C) was drilled on the inner part of the Yermak Plateau in an area with coordinates of 80°27′ N and 6°58′ E. Their average penetration depth is 566 m (B1 in Fig. 1). The maximum penetration depth in sediments is 507.4 mbsf. The sediments belong to a single lithological unit composed of compact homogeneous silty clays and clayey silts more consolidated in surface layers. Detrital material occurs up to a depth of 208.7 mbsf; below this level, it is relatively rare. Three distinguishable subunits differ from each other by changes in the content of detrital material and quartz. Some intervals of the section include rounded siliceous microfossils, rare fragments of molluscan shells, and wood fragments. Carbon concentrations are low (1.5–6.0%); organic carbon is detected throughout the entire section in concentrations of 0.7 to 1.4%. Calcareous nannofossils and planktonic foraminifers occur sporadically in the upper 60–100 m of Quaternary sediments, which are underlain by a thick Pliocene sequence to a depth of 507.4 mbsf. Below 360 mbsf, benthic foraminifers reflect gradual shallowing of the drilling area during the Pliocene. Terrestrial plant remains and palynomorphs are recorded throughout the entire drilled section.

The methane content varies through the section from 10000 to 100000 ppm. Similar ethane and propane concentrations are observable below 300 mbsf. The sharp increase in density (from 1.7 to 2.2 g/cm$^3$) and decrease in porosity (from 50 to 30%) of sediments between 0 and 20 mbsf indicate that the surface sediments are overcompacted, which could be caused by the load of shelf ice.

Site 911 (Holes 911A–911C) is located in the southern shallow-water part of the Yermak Plateau in an area with coordinates of 80°47′ N and 8°23′ E. The average penetration depth of these holes is 902 m. The maximum penetration depth in sediments was 505 mbsf (B2 in Fig. 1). In all three holes, sediments belong to a single lithological unit Pliocene–Quaternary in age composed of unconsolidated clayey silts and silty clays with thin intercalations of clayey and silty mud. Organic remains are rare. Detrital material is more abundant above 340 mbsf, although its rare inclusions are also observable below this level. The rock clasts are represented by siltstones, sandstones, shales, and subordinate coal fragments, igneous rocks, and limestones. The section is characterized by the discrete distribution of Pliocene–Quaternary benthic and planktonic foraminifers and calcareous nannofossils. Siliceous microfossils are extremely rare, represented by recrystallized and reworked specimens. The section exhibits readily definable paleomagnetic Brunhes, Matuyama, and Gauss chrons as well as the Jaramillo and Olduvai subchrons.

The boundary between Quaternary and Pliocene sediments is located at depths of 240 mbsf. The sedimentation rates vary from 170 m/myr in the Pliocene to approximately 100 m/myr during the last million years. The upper 50 m of the section show a certain increase in the degree of sediment compaction, although less notable as compared with that at Site 910. The free methane concentration is high through the entire section.

Site 912 (Holes 912A–912C) is located in the southwestern part of the Yermak Plateau in the area with coordinates of 80°47′ N and 8°23′ E and 79°97′ N, 5°45′ E. The average penetration depth of these holes is 1037 m. The maximum penetration depth in sediments was 145 mbsf in Hole 912A, 40 mbsf in Hole 912B, and 209.1 mbsf in Hole 912C (B3 in Fig. 1). The sediments belong to a single, Pliocene–Quaternary unit represented by unconsolidated clayey silts and silty clays with thin intercalations of clayey and silty mud characterized by weak banded coloration and more abundant detrital inclusions as compared with holes 910 and 911. The sedimentation rates vary from 80 to 100 m/myr decreasing to 30 m/myr during the last million years. Similar sediments were drilled by the D/V *JOIDES* Resolution at Site 986 (Holes 985A–985D) in the Atlantic peripheral part of Spitsbergen [28].

Recently, the sedimentary cover of this region was subjected to extensive investigations by the continuous seismic profiling method [11, 13–15, 19–21, 24] with the integral length of seismic profiles over 5000 km. According to these data, the sedimentary sequence can be divided into several layers (Fig. 2), the numeration and designation of which depends on the study area. In this work, when names of areas or sedimentary layers are not anonymously accepted, we indicate in parentheses their English designations from publications: (YP) Yermak Plateau, (DB) Danskoya Basin, (NoB) Norskebanke, (NA) Nordaustlandet area, (KV) Kvitoya (Kavitoya) Island area, (NB) Nansen Basin, (T) Nansen Basin and Honlopen margin, (SB) Sophia Basin, (B1, B2, B3) ODP holes, (G) Barents Sea.

The uppermost (YP3, SB-3, DB3, NoB2, NA3, KV3, NB3–NB4, T2, GIII–GI, IA) layer is readily correlative in different areas ([11, 14, 15, etc.]) and characterized by a relatively constant thickness of a

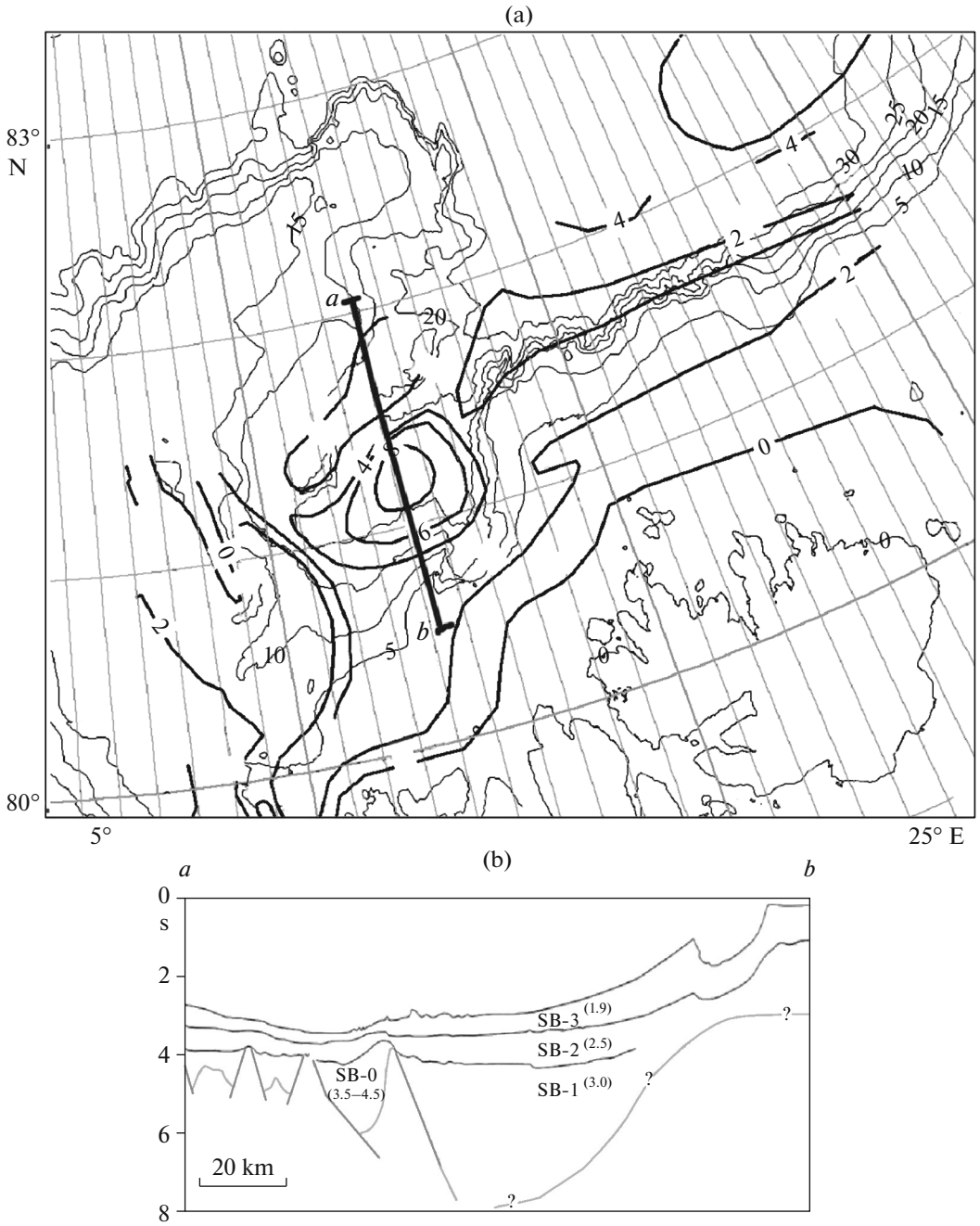


**Fig. 2.** Isopach map (a) and sedimentary section along line *a*–*b* (b) based on data from [14, 24]. For sediments of layers SB-0, SB-1, SB-2, and SB-3, P wave velocities (km/s) are given in parentheses. Isobaths and isopachs are given in hundreds of meters and kilometers, respectively.

0.1–0.2 s two-way travel time through different areas (Fig. 2). It is underlain by the (YP2, SB2, DB2, NA2, KV2, NB2, T2) layer, which is from 0.2 to 0.3 s thick and also reliably correlated between different study areas ([11, 14, etc.]). The base of the NoB-2 layer in the Norskebanke area is located approximately twice as deep compared to bases of other above-mentioned seismostratigraphic units. The thickness of the deepest layer (YP1, SB1, DB1, NoB1, NA1, KV1, NB1, T1) is up to a 0.4 s two-way travel time thick and demonstrates lateral variations. In some areas, it fills depressions in the acoustic basement (Fig 2b). In [11], layer YP0 up to a 0.1 s two-way travel time is defined in the basal part of the sedimentary section.

At the same time, some inconsistencies in identifying sedimentary units in the same areas should be noted. For example, seismic units NB3–NB4 and NB–B1 on the northern slope of the Yermak Plateau defined in [11] correspond to units NB1 and NB3 in [21].

Interpretation of seismic data [11, 14, 15, 19, 20, 24] made it possible to refine the main views on the velocity section of corresponding sediments. This can be exemplified by layers reliably definable on the Yermak Plateau and in neighboring areas from data obtained by a wide-angle seismic survey and acoustic buoy stations. According to these data, layer Yp3 is composed of unconsolidated surface sediments with P wave velocities of 1.7–2.2 km/s. It is underlain by sediments of layer Yp2 compacted by diagenetic processes with P wave velocities up to 3 km/s. Layer Yp1 consists of compact metamorphosed sediments characterized by velocities ranging from 3 to 5 km/s.

The deep-sea holes drilled in areas covered by the seismic profiling survey and other geological data available in publications allow the composition of sediments and their age to be estimated [11, 14, 15, 19, 20, 24]. Layer Yp3 is composed of Pleistocene mud with its lower boundary dated back to 2.6 Ma, no older. Layer Yp2 consists of clayey mud and its base is 6–7 Ma in age, no older. Layer Yp1 is represented by metamorphosed clays dated at 18–35 Ma (or older). Comprehensive interpretation of data on the sedimentary sequence indicates that sedimentation in this area was characterized by different rates. Sediments of layer Yp0 are represented by both marine and terrestrial eolian, lacustrine, and riverine facies. Its base may be relatively old in age.

The available data [11, 14, 15, 19, 20, 24) make it possible to estimate the total thickness of the sedimentary sequence (Fig. 2a). According to these estimates, the thickness of sediments in the southwestern part of the Nansen Basin near its junction with the Sophia Basin exceeds 1 km to reach 4 km locally. In the eastern part of the Sophia Basin near the sublatitudinal rise, which borders the Litke Trough in the south, their thickness decreases from 3 to 1 km. At the same time, south of this rise, there is an isometric depocenter with sedimentary fill up to 8 km thick (and even thicker). To the south, it is augmented by two local depocenters with sedimentary cover up to 4 km thick. Further west, isopachs gradually acquire a submeridional strike and the thickness of sediments never exceeds 1–3 km.

The base of the sedimentary cover in the Eurasia Basin near Spitsbergen has an irregular topography with relative amplitudes of some morphostructures amounting to many hundreds of meters. The seismic data obtained by the CMP method and wide-angle seismic profiling indicate that the acoustic basement underlying the sedimentary cover is crossed by many faults, along which blocks of the Spitsbergen continental slope slide successively relative to each other (e.g., [11, 14, 30, 31, 37, etc.]). The bedding patterns of sedimentary layers in shelf areas of Spitzbergen ([19, etc.]) suggest most likely that intense movements in the basement took place in the Late Paleocene–Early Eocene, while Oligocene and Miocene sediments, which successively overlie each other with conformable boundaries, indicate that notable tectonic movements terminated by that time. The basement is characterized by a complex inner structure with reflectors observable in the depth interval of a 4–8 s two-way travel time.

The availability of deep-sea drilling data from areas covered by the wide-angle seismic survey by buoy stations and other geological information in [11, 14, 15, 19, 20, 24] provide grounds for interpreting the composition of crustal layers and their geometry for areas of the Nansen Basin adjacent to the Sophia Basin. The P wave velocities in the surface layers of the basement are close to 5.2 km/s. In areas with continental crust, reflectors attributed to the granite layer exhibit velocities of almost 6.2 km/s, while in areas underlain by the oceanic crust, they are close to 7 km/s at comparable depths corresponding to the basaltic layer. The complete section of the crust was obtained for five seismic sounding points [11, 24]. The mantle rocks in these areas are characterized by P wave velocities of 8.2 km/s. In areas with oceanic and continental types of the crust, its base is located at depths close to 10 km and deeper than 30 km, respectively.

According to ([29, 33, etc.]), heat flow values in the Eurasia Basin areas adjacent to Spitzbergen can be as high as many hundreds of corresponding units, while west of them, they never exceed 40–90 mW/m$^2$, increasing beneath the Atlantic slope of the Yermak Plateau up to 100–130 mW/m$^2$. The distribution of heat flow values through the study region indicate the SE–NW strike of its minimum located in the area with coordinates 80°–83° N and 5°–15° E corresponding to the central and eastern parts of the Yermak Plateau and Sophia Basin.

The anomalous gravity field in the Faye reduction (Fig. 3a) is characterized by the presence of positive anomalies with absolute values up to 50–150 mGal coinciding with bottom rises and islands [24]. Its negative anomalies with absolute values amounting to ~80 mGal correspond to known basins. Therefore, noteworthy is an arcuate band of negative anomalies extending from the base of the Nordaustlandet continental slope to the northwest direction including the Litke Trough. The easternmost part of the Yermak Plateau (which subsided to water depths of 1.5 km) is separated from its western part (with a water depth up to 0.5 km) by an area with the lowered (close to zero) values of the gravity field.

The anomalous gravity field in the Bouguer reduction (Fig. 3b) is characterized by the presence of positive anomalies with absolute values up to 200 mGal. Negative anomalies with absolute values up to ~30 mGal are related to islands and continental shelves. The Yermak Plateau is generally characterized by a low-anomalous gravity field with almost zero values.

Thorough analysis of the data on the physical rock properties in [18, 26, 33, 36, etc.] reveals correlation between P wave velocities (km/s) and density (g/cm$^3$)

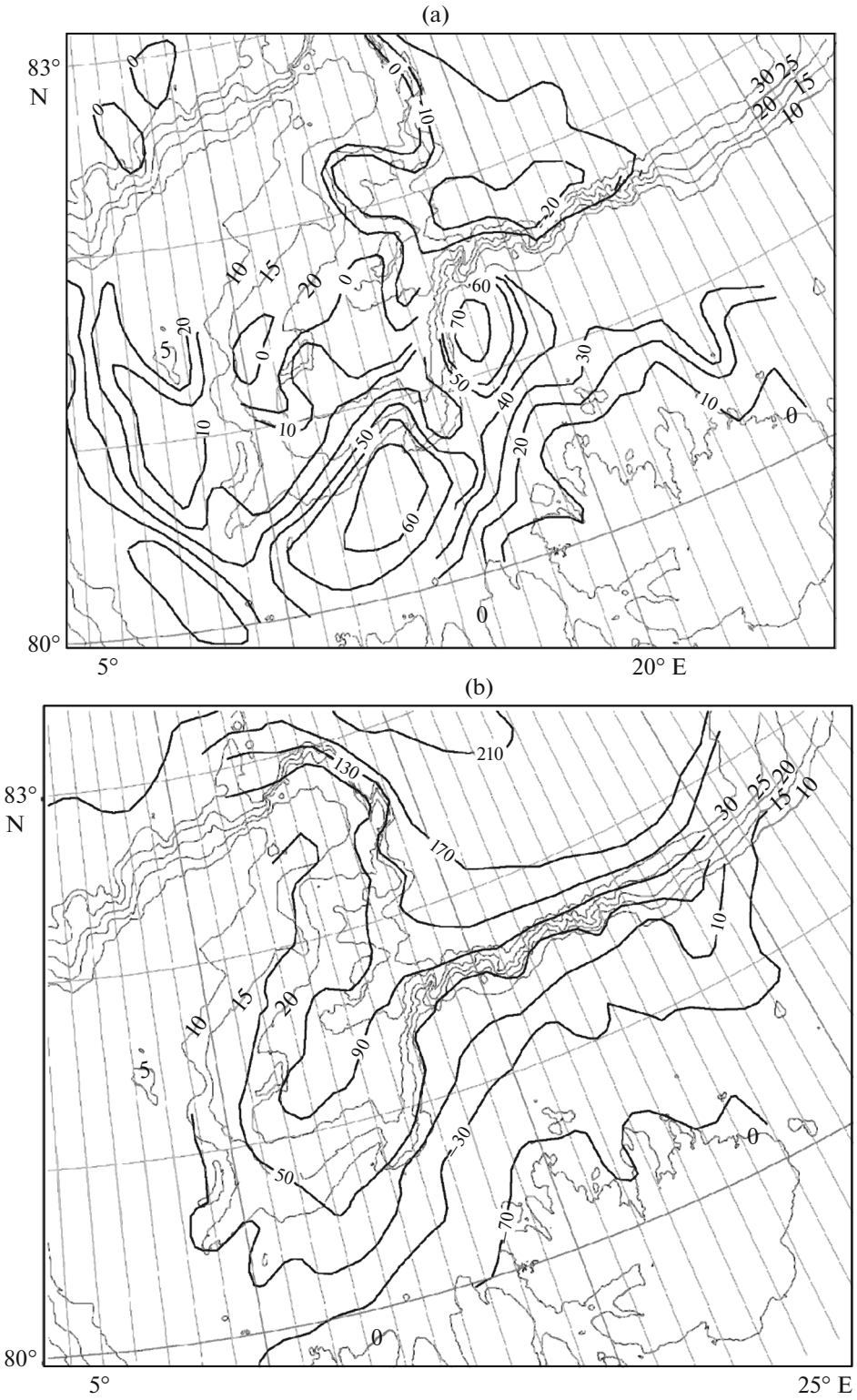


**Fig. 3.** Faye (a) and Bouguer (b) gravity anomalies, after [24] simplified. Isobaths and isoanomals are given in hundreds of meters and milligals, respectively.

of rocks. For the area under consideration, such a correction made it possible to establish that sedimentary rocks with P wave velocities of 1.8–2.0, 2.3–3.0, and 3.3–3.8 km/s are characterized by densities of 1.8–2.0, 2.1–2.2, and 2.4 g/cm$^3$, respectively. In the above-cited works, the upper part of the consolidated continental crust and lower layers of the oceanic crust are considered as being characterized by densities of

2.6–2.7 and 2.9 g/cm$^3$, respectively. The density of the upper mantle is accepted in calculations as ranging from 3.1 to 3.3 g/cm$^3$.

The data on densities of lithospheric layers taken into account in comprehensive interpretation of the gravity field in the Bouguer reduction made it possible to compile several sections, which characterize crust of particular types in the study region [14, 19, 24]. As follows from these sections, the segment of the deep-sea Nansen Basin adjacent to Spitsbergen and the Sophia Basin is underlain by oceanic crust approximately 10 km thick with a thick (up to 2–3 km) sedimentary layer. The depths of the Moho interface vary from 12 to 14 km, increasing toward the shelf with continental crust up to 32–34 km. In the central part of the Yermak Plateau, the Moho discontinuity is located at depths of approximately 25 km [14]. In the last work, its authors present a schematic map illustrating the distribution of the crust transitional from continental to oceanic type. It mainly covers the outer shelf, slope, and its base in the eastern area of the Spitsbergen Archipelago. Similar results are also available in [6].

According to aeromagnetic observations ([4, 7–9, 32, 34, 35, etc.]), magnetic anomalies in the Eurasia Basin south of the axis of the Mid-Arctic Ridge vary from 30 to 500 nT with an average wavelength of 10–40 km. Comparison of the observed and theoretical magnetic anomalies in the bottom spreading model allowed paleomagnetic anomalies older than C13 to be identified in the Nansen Basin adjacent to Spitsbergen. The oldest anomalies are C24 ([1, 24, 36, etc.]), C24B ([10, 11, etc.]), and C25 ([4, etc.]). It means that the oldest chron should be coeval with Chron C25o in the Greenland part of the Eurasia Basin [7]. Therefore, in this work, the nameless chron in the Spitsbergen part of the Eurasia Basin is designated as C25o. In such conditions, the spreading rate should be approximately 1 cm/yr. In some works, linear magnetic anomalies in the Nansen Basin (e.g., the unnamed paleoanomaly in [36], C13 in [34], C20 in [12], C20 in [17], and C18 and C20 in [1] continue to the eastern peripheral and even central parts of the Yermak Plateau.

The magnetic field of the Sophia Basin has been intensely investigated in recent decades. According to some researchers, there are no linear magnetic anomalies in the basin ([4, 11, 36, etc.]). At the same time, other authors (e.g. [12, etc.]) show in their works the position of the abandoned rift passing along the axial part of the basin and continuing via the Sophia trough to the Sverdrup Bank. There are also works in which the Sophia Basin is characterized by linear magnetic anomalies of spreading origin (e.g., [17, etc.]). The oldest and youngest paleomagnetic anomalies are C24 [17, 36] and C21 [17], respectively. In addition, paleoanomaly C22 is traceable from the Nansen Basin to the central part of the basin in question [17]. Changes in the magnetic field in the western part of the Nansen Basin [4, 7] gave grounds for outlining the boundary or transitional zone between the continental and oceanic crust [1], which was confirmed by the comprehensive interpretation of the data obtained by the wide-angle seismic profiling survey [24]. In works [11, 14, 25], this boundary (or zone) extends to the Sophia Basin occupying either its peripheral part ([11, 14, etc.]) or entire basin (the Yermak Plateau included) [25].

If the bottom of the basin was formed by spreading, it should have a corresponding axis. A potential candidate for representing such a spreading axis may be paleoanomaly C22. In this case, paleoanomaly C21 defined near the base of the southern slope of the Yermak Plateau should be coeval with paleoanomaly C24 near the northern continental slope of Spitzbergen and should be reidentified as C24. Our electronic database contains data obtained by the aeromagnetic survey of the Naval Research Laboratory (NRL, USA) in 1998–1999 for the western half of the Eurasia Basin, which were published in 2003 [7]. Figure 4a shows a compiled schematic map of magnetic chronology of the Eurasia Basin bottom near Spitsbergen. Analysis of these data along particular observation profiles reveals no presence of magnetic anomalies extending for tens of kilometers in the Sophia Basin, which would allow any linear magnetic anomalies of spreading origin to be identified.

## DISCUSSION

As follows from comprehensive interpretation of available geological and geophysical data, the Yermak Plateau [13–15] (or its western part) represents a continental fragment separated from the Spitsbergen domain of the Eurasian continent during the formation of the Eurasia Basin. This inference and impossibility of defining linear magnetic anomalies in the Sophia Basin give grounds to assume that the latter resulted from separation of the Yermak Plateau from the Spitsbergen continental slope. This process was most likely preceded by significant extension of the continental crust in the primary junction zone between the Spitsbergen and Yermak Plateau blocks. This instigated the slide of continental crust fragments along the plane of the crustal-penetrating fault. The sliding fragments of the upper consolidated crust in the Sophia Basin are reported from the sedimentary cover by ([11, 14, etc.]. In our opinion, their slide proceeded in accordance with the model in [38] and mechanism described in detail in [5]. The initial position of such fragments was reconstructed by calculation of the Euler poles and angles of rotation using original programs developed at the Laboratory of Geophysics and Tectonics of the Ocean Bottom (Institute of Oceanology, Russian Academy of Sciences) incorporated into the Global Mapper software environment [5]. The calculation technique is discussed in [2]. For brevity, we call pairs of isobaths on

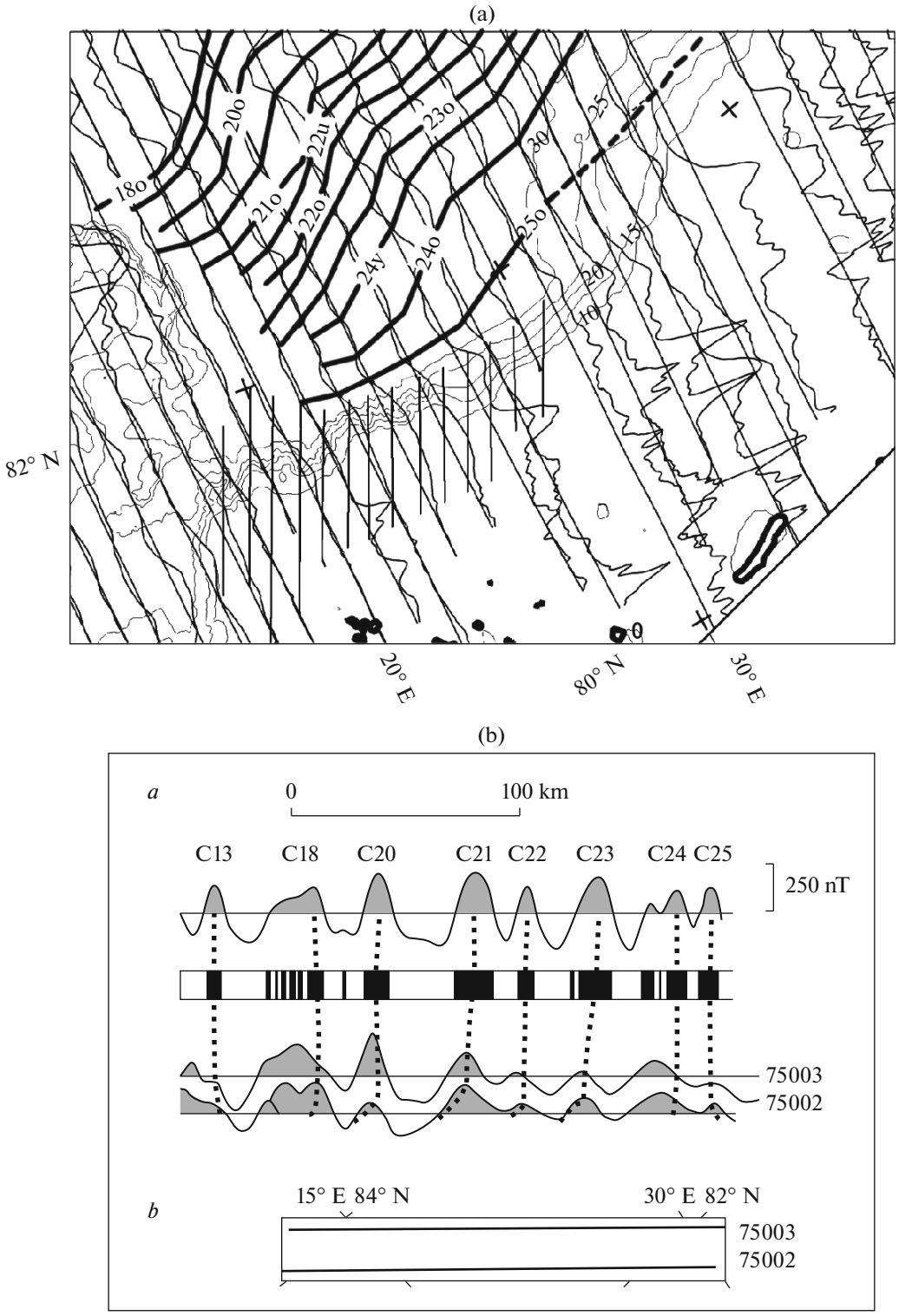


**Fig. 4.** (a) profiles of anomalous magnetic field, chrons (heavy lines), and transitional zone between oceanic and continental crust (hachured). Isobaths are given in hundreds of meters. (b) Theoretical paleoanomalies in model of inverse magnetically active layer and correlation of paleoanomalies C13–C25 along profiles 7503 and 7503 (a); their position is shown in inset (b). Based on data from [4, 7, 14, 27] and geochronological scale from [16].

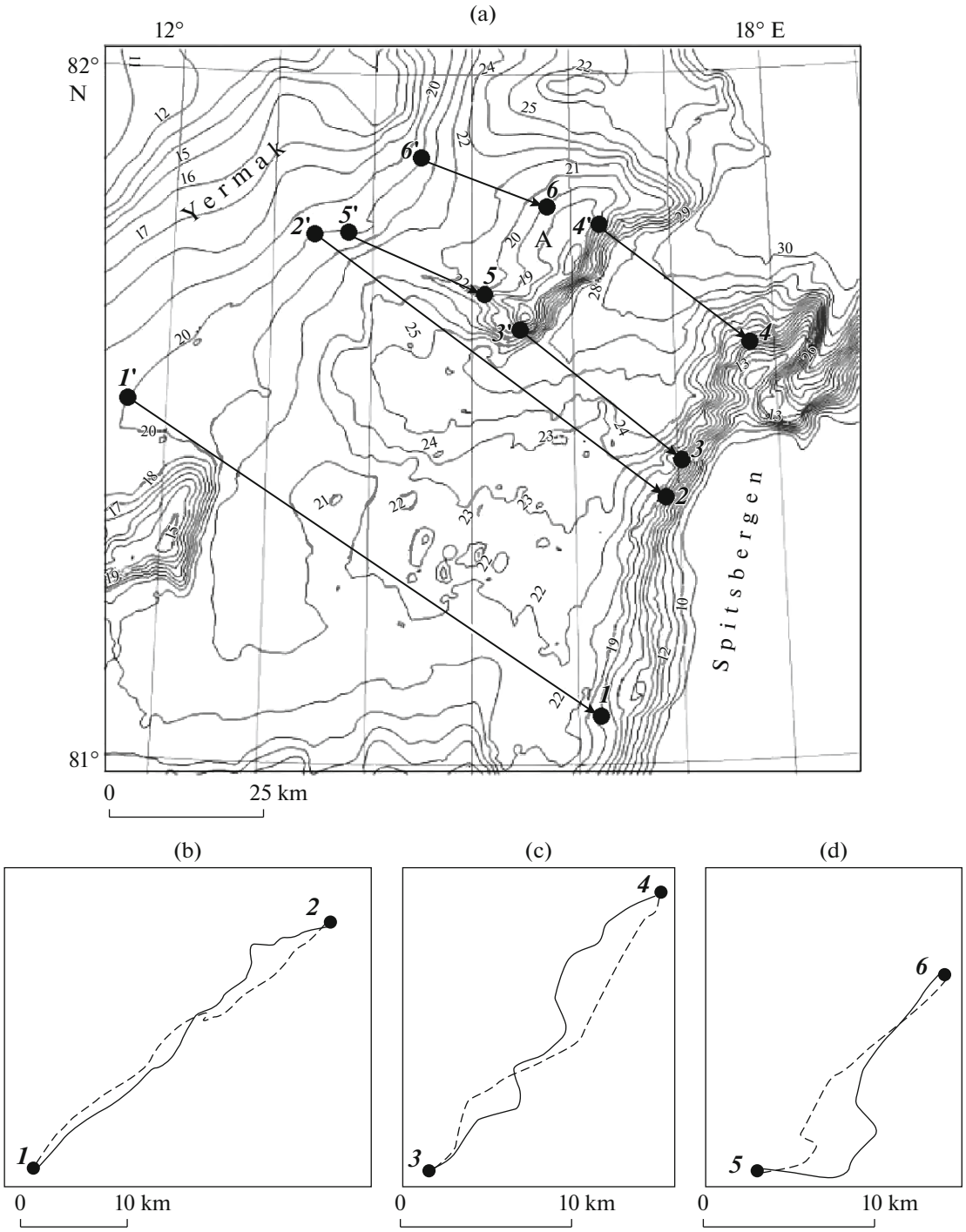


**Fig. 5.** (a) Position of end points *1–4* in conjugate isobaths of Spitsbergen Island, ***5–6*** and ***3'–4'*** of rise A, ***1'–2'*** and ***5'–6'*** of the Yermak Plateau. Straight lines with arrows indicate conjugate points in different areas: (b) Spitsbergen (1.9 km isobath, solid line) and Yermak Plateau (2.0 km isobath, dashed line, (c) Spitsbergen (1.9 km isobath, solid line) and southern slope of the rise A (2.0 km isobath, dashed line), (d) northern slope of rise A (2.0 km isobath, solid line) and Yermak Plateau (2.1 km isobath, dashed line). Points *1–6* in (b), (c), and (d) are same as in (a). Isobaths are given in hundreds of meters.

opposite slopes selected for geodynamic calculation conjugate isobaths.

According to calculations, the position of the Euler pole at the point with coordinates 81.84° N and 14.86° W provides relatively good fitting of the 1.9 km isobath in the lower part of the Spitsbergen slope (the rea between points ***1*** and ***2*** in Figs. 5a and 5b) and the 2.0 km isobath of the Yermak Plateau (the area between points ***1'***and ***2'***) for a distance of 50 km north of 80°. The angle of rotation was 12.9° ± 0.3° and the mean-square devia-

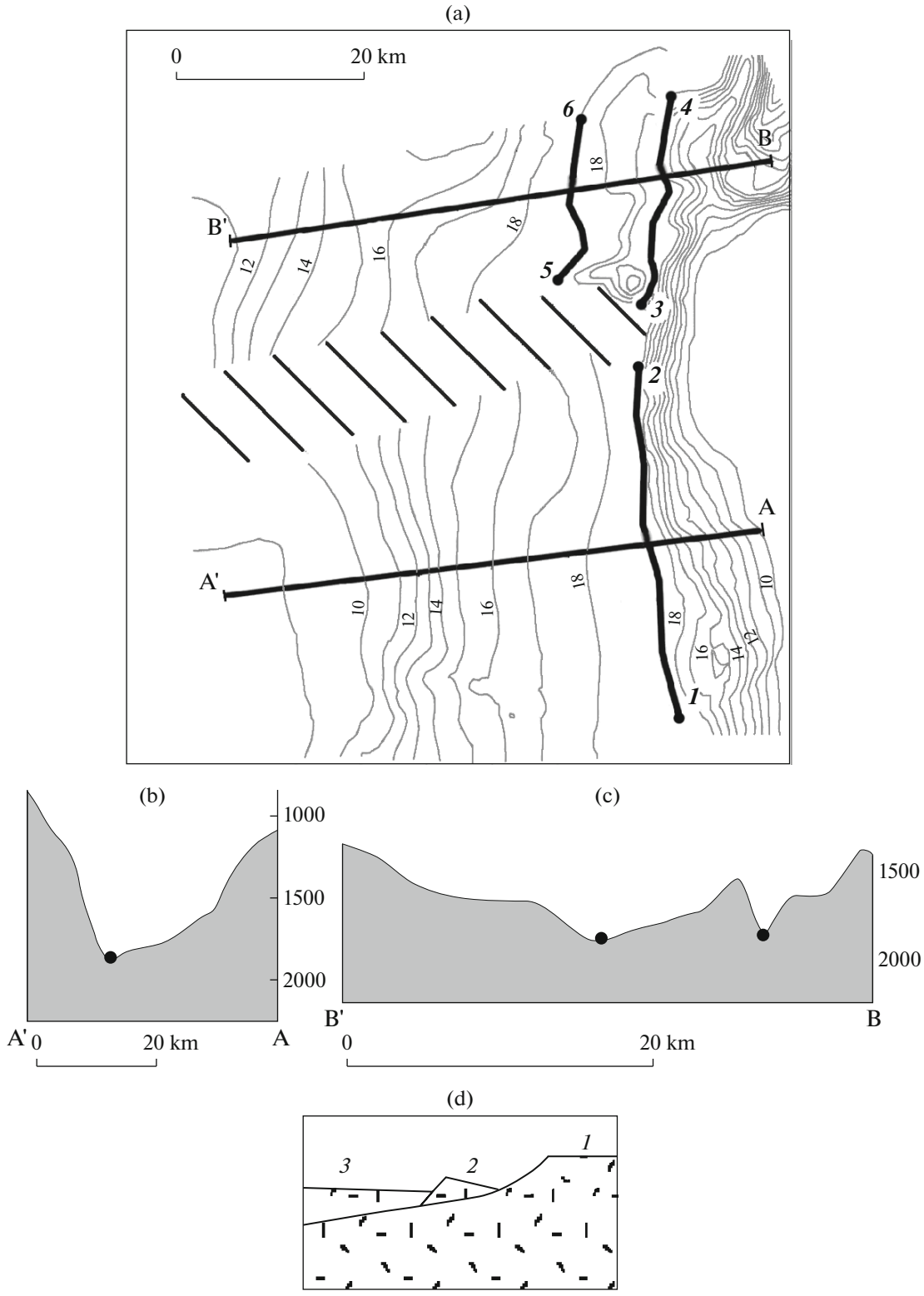


**Fig. 6.** Paleogeodynamic reconstruction of fitness between opposite slopes using conjugate isobaths and reconstructed paleobathymetry. Segments of heavy curved line and hatching designate axes of splitting zones and tectonic fractures. Points *1*–*6* same as in Fig. 5. Straight lines show paleobathymetric profiles along lines A'–A (b) and B'–B (c) prior to separation of two continental fragments from Spitsbergen and points of paleoisobath conjugation. Figure 4d demonstrates model of sliding blocks along profile B'–B: (*1*) Spitsbergen Island, (*2*) rise A based on data from Fig. 5a, (*3*) Yermak Plateau.

tions in calculated conjugate points were ±4 km (5 conjugate points).

Rise A and the Spitzbergen slope are separated from each other by a basin approximately 20 km wide and up to 3.3 km deep (the area between conjugate points ***3***, ***4***, ***3'***, ***4'*** in Figs. 5a and 5b). If it is accepted that the formation of this basin is related, in accordance with the model in [38], to the sliding of one of the continental crust blocks along the continental slope of Spitsbergen, 1.9 km isobath in the lower part of the Spitsbergen slope (between points ***3*** and ***4*** in Figs. 5a and 5b) and the 2.0 km isobath in rise A (between points ***3'*** and ***4'***) appear the most suitable for paleogeodynamic analysis. The conjugation itself described by the Euler pole with rotation of different and the same isobaths demonstrates that the most suitable for paelogeodynamic analysis are the segments of the 2.0 isobath in the lower part of rise A (between points ***5*** and ***6*** in Figs. 5a and 5b) and the 2.1 km isobath in the Yermak Plateau area (between points ***5'*** and ***6'***). The conjugation is described by the Euler pole located in the area with coordinates 81.6° N and 15.27° W with a rotation angle of 4.7°. The mean-square deviation in the calculated conjugate points was ±6 km (5 points).

The calculations made it possible to reconstruct the axes of splitting zones between peripheral continental fragments of Spitsbergen and its main block (heavy lines ***1–2***, ***3–4***, ***5–6*** in Fig. 6a). An important feature of the reconstruction is the establishment of the difference in depth of conjugate isobaths amounting to 100 m. Corrections for the slide of separated continental fragments introduced into the reconstruction made it possible to calculate the bathymetry of the area prior to separation of these sliding fragments (Figs. 6b and 6c). The figures show that peripheral areas of the Yermak Plateau in the Sophia Basin were primarily raised above the main surface of Spitsbergen by a hundred meters. Figure 6d shows the model illustrating the slide of these continental fragments along the crustal-penetrating fault.

## CONCLUSIONS

Our investigations revealed that prior to extension of the lithosphere in the Eurasia Basin, the Yermak Plateau was an element of the Arctic Eurasian margin. Extension in the Barents Sea shelf graded with time into rifting, which resulted in separation of this continental fragment from the main continent 57.656–59.237 Ma ago (Chrons C25r–C26n). This process was accompanied by the emplacement of many basic dikes, which could determine the formation of high-amplitude magnetic anomalies in the Yermak Plateau area. Our reconstruction of axes in the splitting zones along peripheral continental fragments of Spitsbergen and determination of the Euler poles and angles of rotation made it possible to interpret the kinematics of this process. It was revealed that the difference between the depths of conjugate isobaths can be as large as many tens of meters, which reflects the different-scale slide of peripheral areas of the continental crust along the plane of the crustal-penetrating fault and, correspondingly, their different subsidence during rifting. A model illustrating the slide of these continental blocks proposed and a model illustrating the slide of these continental blocks are proposed.

## ACKNOWLEDGMENTS

This work was supported by a State Contract no. 0149-2014-0030 and partly by the Russian Foundation for Basic Research (project no. 14-08-00015).

## REFERENCES

1. V. Yu. Glebovsky, V. D. Kaminsky, A. N. Minakov, S. A. Merkur'ev, V. A. Childers, and J. M. Brozena, "Formation of the Eurasia basin in the arctic ocean as inferred from geohistorical analysis of the anomalous magnetic field," Geotectonics **40** (4), 263–281 (2006).
2. D. D. Zonenshtein, M. G. Lomize, and A. G. Ryabukhin, *Practical Manual on Geotectonics* (Moscow State University, Moscow, 1990) [in Russian].
3. N. I. Filatova and V. E. Khain, "The Arctida Craton and Neoproterozoic-Mesozoic orogenic belts of the circum-polar region," Geotectonics **44** (3), 203–227 (2010).
4. A. A. Schreider, "Linear magnetic anomalies in the Arctic Ocean," Oceanology (Engl. Transl.) **44** (5), 721–729 (2004).
5. Al. A. Schreider, "Model of the separation of the Marvin Spur from the Lomonosov Ridge in the Arctic Ocean," Oceanology (Engl. Transl.) **54** (4), 490–496 (2014).
6. A. Alvey, C. Gaina, N. Kuszner, and T. Torsvik, "Integrated crustal thickness mapping and plate reconstructions for the high Arctic," Earth Planet. Sci. Lett. **274**, 310–321 (2008).
7. J. Brozena, V. Childers, L. Lawver, et al., "New aerogeophysical study of the Eurasian Basin and Lomonosov Ridge implications for basin development," Geology **31**, 825–828 (2003).
8. R. Coles and P. Taylor, "Magnetic anomalies," in *Geology of North America* (Geological Society of America, Boulder, CO, 1990), **Vol. 1**, pp. 119–132.
9. A. Dore, E. Lundin, N. Kusznir, and C. Pascal, "Potential mechanisms for the genesis of Cenozoic domal structures on the NE Atlantic margins," Geol. Soc. London Spec. Publ. **306**, 1–26 (2008).
10. A. Dossing, L. Stemmerik, T. Dahl-Jensen, and V. Schlindwein, "Segmentation of the eastern north Greenland oblique shear margin-regional plate tectonic implications," Earth Planet. Sci. Lett. **292**, 239–253 (2010).
11. O. Engen, J. A. Gjengedal, J. Faleide, et al., "Seismic stratigraphy and sediment thickness of the Nansen basin, Arctic Ocean," Geophys. J. Int. **176**, 805–821 (2009).

12. O. Engen, J. Faleide, and T. Dyreng, "Opening of the Fram Strait gateway: a review of plate tectonic constraints," Tectonophysics **450**, 51–69 (2008).
13. O. Engen, J. I. Faleide, F. Tsikalas, et al., "Structure of the west and north Svalbard margins in a plate tectonic setting," in *Proceedings of the 4th International Conference on Arctic Margins* (Dartmouth, Canada, 2003), p. 40.
14. W. Geissler and W. Jokat, "A geophysical study of the northern Svalbard continental margin," Geophys. J. Int. **158**, 50–66 (2004).
15. W. Geissler, W. Jokat, and H. Brekke, "The Yermak plateau in the Arctic ocean in the light of reflection seismic data – implication for its tectonic and sedimentary evolution," Geophys. J. Int. **187**, 1334–1362 (2011).
16. F. Gradstein, J. Ogg, M. Schmitz, and G. Ogg, *The Geologic Timescale 2012* (Elsevier, Amsterdam, 2012).
17. H. Jackson and G. Johnson, "Summary of arctic geophysics," J. Geodyn. **6**, 245–262 (1986).
18. W. Jokat and U. Micksch, "The sedimentary structure of Nansen and Amundsen basins, Arctic Ocean," Geophys. Res. Lett. **31**, L02603 (2004). doi 10.1029/2003/GL018352
19. J. Knies, J. Matthiessen, C. Vogt, et al., "The Plio-Pleistocene glaciation of the Barents Sea–Svalbard region: a new model based on revised chronostratigraphy," Quat. Sci. Rev. **28**, 812–829 (2009).
20. J. Knies, J. Matthiessen, K. Fabian, et al., "Effect of early Pliocene uplift on late Pliocene cooling in the Arctic-Atlantic gateway," Earth Planet. Sci. Lett. **387**, 132–144 (2014).
21. Y. Kristoffersen and E. Husebye, "Multi-channel seismic reflection measurements in the Eurasian Basin, Arctic Ocean, from U.S. ice station FRAM-IV," Tectonophysics **114**, 103–115 (1985).
22. L. Lawver, A. Grantz, and L. Gahagan, "Plate kinematic evolution of the present Arctic region since the Ordovician," Geol. Soc. Am. Spec. Pap. **360**, 333–358 (2002).
23. N. Lebedeva-Ivanova, *Geophysical Studies Bearing on the Origin of the Arctic Ocean Digital Comprehensive Summaries of Uppsala Dissertations from the Faculty of Science and Technology* (Uppsala University, Uppsala, 2010).
24. A. Minakov, J. Faleide, V. Glebovsky, and R. Mjelde, "Structure and evolution of the northern Barents Kara sea continental margin from integrated analysis of potential fields, bathymetry and sparse seismical data," Geophys. J. Int. **188**, 79–102 (2012).
25. J. Mosar, G. Lewis, and T. Torsvik, "North Atlantic seafloor spreading rates: implication for the tertiary development of inversion structures of the Norwegian–Greenland Sea," J. Geol. Soc. London **159**, 503–515 (2002).
26. J. Nafe and C. Drake, "Variation with depth in shallow and deep water marine sediments of porosity, density and the velocity of compressional and shear waves," Geophysics **22**, 523–552 (1957).
27. *Ocean Drilling Program Initial Report Leg 151* (College Station, TX, 1995).
28. *Ocean Drilling Program Initial Report Leg* (College Station, TX, 1999).
29. N. Okay and K. Crane, "Thermal rejuvenation of the Ermak plateau," Mar. Geophys. Res. **15**, 243–263 (1993).
30. O. Ritzmann and W. Jokat, "Crustal structure of northwestern Svalbard and the adjacent Yermak Plateau: evidence for Oligocene detachment tectonics and non-volcanic breakup," Geophys. J. Int. **152**, 139–159 (2003).
31. O. Ritzmann, W. Jokat, W. Czuba, et al., "A deep seismic transect from Hovgard Ridge to northwestern Svalbard across the continental-ocean transition: a sheared margin study," Geophys. J. Int. **157**, 683–702 (2004).
32. P. Taylor, L. Kovacs, P. Vogt, and G. Johnson, "Detailed aeromagnetic investigations of the Arctic Basin," J. Geophys. Res. **86**, 6323–6333 (1981).
33. M. Urlaub, M. Schmidt-Aursch, W. Jokat, and N. Kaul, "Gravity crustal models and heat flow measurements for the Eurasia basin, Arctic ocean," Mar. Geophys. Res. **30**, 277–292 (2009).
34. P. Vogt, "Magnetic anomalies and crustal magnetization," in *The Western North Atlantic Region* (Geological Society of America, Boulder, CO, 1986), pp. 229–256.
35. P. Vogt, P. Taylor, L. Kovacs, and G. Johnson, "Detailed aeromagnetic investigation of the Arctic Basin," J. Geophys. Res. **84**, 1071–1089 (1979).
36. E. Weigelt and W. Jokat, "Peculiarities of roughness and thickness of oceanic crust in the Eurasia Basin, Arctic Ocean," Geophys. J. Int. **145**, 505–516 (2001).
37. D. Winkelmann, W. Jokat, F. Niessen, et al., "Age and extent of the Yermak slide north of Spitsbergen, Arctic Ocean," Geochem. Geophys. Geosyst. **7** (6), Q06007 (2006). doi 10.1029/2005GC001130
38. B. Wernicke, "Low angle normal faults in the Basin and Range Province: nape tectonics in an extending orogeny," Nature **291**, 645–648 (1981).
39. Satellite geodesy, International bathymetric chart of the Arctic Ocean, 2014. http://www.topex.ucsd.edu/html/mar_topo.html.

*Translated by I. Basov*